How Plausible is getting Ferromagnetic Interactions by Coupling Blatter's Radical via its Fused Benzene Ring?

Rishu Khurana, Ashima Bajaj, and Md. Ehesan Ali*

Institute of Nano Science and Technology, Phase 10, Sector-64, Mohali Punjab-160062, India

E-mail: ehesan.ali@inst.ac.in

Abstract

With ongoing efforts to synthesize super-stable Blatter's diradicals having strong ferromagnetic exchange interactions, all the ten possible isomers of di-Blatter diradical coupled through the fused benzene rings are investigated. A variety of electronic structure theory such as broken-symmetry methods in density functional theory (DFT), spin-constraint DFT (CDFT), and wave function-based multi-configurational methods e.g. CASSCF/NEVPT2 are applied to compute the magnetic exchange interactions. Surprisingly, anti-ferromagnetic interactions are revealed for all the stable isomers of di-Blatter diradicals. Indeed it commensurates with the experimental observations for the only available synthesized isomer. However, the other nine isomeric diradicals in the series are yet to synthesize. Despite a good match between theory and experiment, the anti-ferromagnetic exchange interactions could not be explained based on the *spin alternation* rule due to unique spin-distributions in the triazinyl ring. Thus, we propose the *zonal spin-alternation* rule which explains the observed ground spin-state for the conjugated di-Blatter diradicals quite accurately. Further, the fractional spin-moment localization on the N-atoms activates multiple exchange pathways and the dominating exchange interactions render anti-ferromagnetic interactions in the conjugated isomers. The study further reveals that due to strong steric hindrance in certain coupled isomers, the exchange interaction switches from anti-ferromagnetic to weak ferromagnetic interactions with the cost of stabilization energy of the radicals. Thus it questions the possibility of synthesizing ferromagnetic di-Blatter diradicals.

1 Introduction

An emerging interest for organic molecular magnets (OMMs) in the fabrication of spintronic devices has eventually thrusts into investigation of thermally stable organic radicals.[1,2] Being a fundamental source of spin, organic diradicals have attracted substantial attention of the researchers for potential applications in the field of spintronics as memory storage and logic devices.[3–5] One of the major challenge faced by the community is obtaining the room temper-

ature stable organic radicals that exhibit strong ferromagnetic exchange interactions. Over the past few decades, a number of stable organic radicals including nitronyl nitroxide(NN), oxoverdazyl (OVER), dithiadiazolyl (DTDA) have been successfully developed.[6–9] One of the other thermally robust monoradical is 1,2,3-benzotriazinyl (Blatter's) radical (shown in Fig. 1), which was first reported by Blatter and co-workers in 1968.[10] The radical has gained considerable attention after Koutentis et al. established easy synthetic strategies for super stable Blatter's radical.[11,12] Afterwards, focusing on electronic and magnetic properties, various magneto-structural correlations were also established by them in the π-stacked radicals of Blatter's radical.[13] Along with this, the radical has witnessed a growing interest with applications in spintronic devices. Ciccullo et al. demonstrated the excellent ability of using a Blatter's radical to create stable thin films, thus, opening the way for the radical to be used in devices.[14] Several recent studies have also examined the stability of Blatter's radicals when interfaced with metallic substrates and conducting electrodes.[15,16] The radical has also found extensive applications in transition metal-radical complexes,[17] optical properties including photocyclization[18] and in context of controlled polymerization.[19] With a biggest challenge to synthesize room temperature stable organic diradicals, Rajca et al. successfully coupled the stable nitronyl nitroxide (NN) as well as imino nitroxide (IN) radical with the Blatter's radical to obtain hybrid diradicals that exhibit reasonably strong ferromagnetic exchange interactions.[20,21] Based on *ab initio* calculations we recently proposed diradicals with strong ferromagnetic interactions by coupling the Blatter's radical with the known stable radicals via the phenyl ring directly connected to N-atom of the triazinyl ring.[22] Recently, Zheng et al. reported the synthesis of diradical obtained by coupling the monomeric unit of Blatter's radical itself.[23,24]

For a diradical, the magnetic exchange interaction between the two unpaired spins residing in the two singly occupied molecular orbitals (SOMOs) leads to either ferromagnetic (parallel) or anti-ferromagnetic (antiparallel) alignment of unpaired spins in the ground state.[25] The nature of the exchange interactions for organic diradicals could be predicted based on

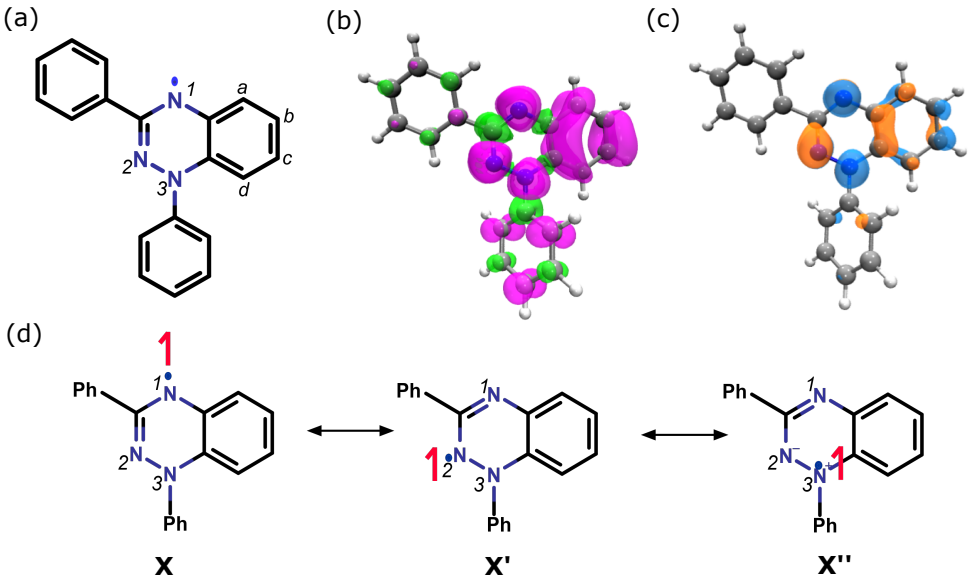

Figure 1: **(a)** Parent 1,2,3-benzotriazinyl (Blatter's) radical, **(b)** Löwdin spin density distribution where pink and green colors represents α and β spin with isovalue 1×10^{-3} $\mu_B/Å^3$ and **(c)** Singly occupied molecular orbital (SOMO) of Blatter's monoradical with isovalue 2×10^{-2} a.u. **(d)** Major contributing resonating structures of Blatter's monoradical indicating the delocalization of unpaired electron on all the three N-atoms.

the *spin alternation* rule which states that even number of conjugated bonds between two spin centres provide ferromagnetic exchange, while antiferromagnetic interactions arise for odd number of bonds.[26] This simple rule works perfectly well in predicting the nature of magnetic exchange interactions for almost all the conjugated diradicals except few special cases where the electronic conjugation of the π-orbitals is broken due to the orthogonal arrangement of the p_z-orbitals of a pair of adjacent C-atoms in the exchange pathway.[27–29]

For Blatter's monoradical, Löwdin spin density distribution, shown in Fig. 1b, reveals that the unpaired electron is not only confined to three N-atoms, but delocalizes across both the triazinyl and fused benzene ring. This unique spin density distribution of the radical makes this super stable spin source an appealing candidate for stable OMMs, further imposing the question, can we couple such mono-radicals to obtain Blatter's diradical with strong ferromagnetic exchange interactions? To find an answer priori to synthesis, in this work, we have computationally investigated the 10 possible isomers of di-Blatter diradical by coupling the monomeric unit of Blatter's radical via its fused benzene ring. Adopting various

density based methods along with the multi-reference CASSCF/NEVPT2 calculations, magnetic exchange interactions are computed and are compared with the available experimental observations. As a peculiarity of Blatter's radical, the fractional spin-moment localization on all the three N-atoms yields multiple micro-magnetic centres. The pairwise exchange between the specific micro-magnetic centres is addressed with appropriate computational recipe.

Further, the Löwdin spin density distribution, shown in Fig. 1b, also reveals that all the N-atoms possess α-spin (positive spin density). Approximate 0.23 μ_{B} spin-moment was found on each of the three N-atoms. Even N3-atom also exhibits α-spin due to resonance contributing structures, shown in Fig 1d, which is in contrast to the empirical *spin alternation* and the similar *Ovchinnikov's* rule where alternate signs of spin density are expected at the adjacent sites.[30] This α-spin cloud over the triazinyl ring itself gives a first signature that simplest *spin alternation* rule cannot be applied to such radicals. Thus, as an alternative way, in this work, we also proposed a modified version of *spin alternation* rule called here as *zonal spin alternation* rule, which can be applied correctly to predict the nature of magnetic exchange interactions in such systems.

2 Theoretical Methods and Computational Details

The magnetic exchange interactions ($2J$) between the two magnetic centres could be represented by Heisenberg-Dirac-Van Vleck spin Hamiltonian

$$\hat{H}_{HDVV} = -2J\hat{S}_1\hat{S}_2 \tag{1}$$

where $\hat{S}_1$ and $\hat{S}_2$ are the spin angular momentum operators on two spin centres. For a diradical, $2J$ could be expressed as the energy difference between the singlet (E_{S}) and triplet (E_{T}) spin state i.e.

$$E_S - E_T = 2J \tag{2}$$

In the single-determinant formalism (e.g. HF, KS), the singlet state of a diradical cannot be represented due to multi-determinantal nature of the low spin-state wave function. However, an alternative route to evaluate $2J$ is the broken-symmetry (BS) approach within DFT framework as proposed by Noodleman.[31] In this approach the $2J$ can be extracted using

$$2J = 2(E_{BS} - E_T)/S^2_{max}, \tag{3}$$

where E_{BS} is the energy of broken-symmetry state. Generally, DFT functionals tend to strongly delocalize the magnetic orbitals which might result in over-prediction of $2J$ values. An alternative approach to this problem is spin-constraint DFT (CBS-DFT) that allow total energy calculations by constraining the spin-magnetic moments on the specified zones.[32,33] The exchange coupling could then be extracted using Eq. 3 with CBS-DFT total energies.[34]

For all the isomers of di-Blatter diradical under study, the molecular geometries are first optimized at UB3LYP/def2-TZVP level. The exchange interactions are then investigated applying different density as well as wave function-based *ab initio* multi-configurational methods.[35–37] All the wave function-based and BS-DFT calculations are performed using *ORCA*[38], while CBS-DFT calculations are performed in *NWChem.*[39] The static as well as dynamical electronic correlations are accounted through CASSCF and the N-electron valence state perturbation theory (NEVPT2) method respectively wherein the $2J$ values are obtained by using Eq. 2.[40,41] The multi-reference (CASSCF/NEVPT2) calculations of $2J$'s are benchmarked for a set of active spaces starting from minimal CAS(2,2) to CAS(6,6) for the experimentally observed **c-c** isomer (see SI). We observed that using the minimum active space (i.e. accounting two SOMOs in the active space) underestimates the static-correlations and results in smaller $2J$ values in the CASSCF method, however, it gets compensated while accounting the dynamical correlations and produce a very close number as observed in the experiments as well as in other theoretical methods. Expanding the active space improves static correlations but overall $2J$ values get overestimated. These scenarios were also observed previously

in the literature.[22,42–44] Considering all these facts, further, all the calculations are performed using CAS(2,2) active space along with the static and dynamic correlations.

3 Results and Discussions

All the possibilities of coupling the Blatter's radical with itself via fused benzene ring are investigated. As illustrated in Fig. 1a, fused benzene ring exhibits four distinct unsubstituted positions (marked as a,b,c and d in Fig. 1a) through which it can be coupled to other Blatter's moiety. So, in total 4×4, i.e. 16 constitutional isomers of di-Blatter diradical can be formed, but 6 of them being repetitive in combination (as **a-b** and **b-a** denotes the same isomer) give rise to 10 possible isomers with distinct atomic connections. Out of these 10 possibilities, isomers obtained by coupling the radical moieties via connecting sites "a" or "d" are sterically hindered with distorted geometry and large torsional angles. On the other hand, coupling via connecting sites "b" or "c" results in nearly planar geometry and less torsional angles. Fig. 2 illustrates the relative energies and the dihedral angle ϕ between two monomeric units optimized at UB3LYP/def2-TZVP level for all the 10 isomers. Among the 10 possibilities, the isomers with connecting sites "b" and "c" ,i.e., **b-b, b-c** and **c-c** are found to be energetically stable exhibiting a dihedral angle of $\sim 35°$ as compared to those with connecting site "a" and "d" exhibiting large dihedral angles. Among the stable isomers, the diradical with mirror connecting cite "c", i.e. **c-c** (shown in inset of Fig. 2) has already been synthesized, however, the other two isomers i.e. **b-b** and **b-c** are also potentially stable candidates and are yet to be synthesized. The magnetic properties of the former were also studied applying SQUID magnetometry by Zheng and co-workers wherein an anti-ferromagnetic exchange with a $2J$ value of -444.19 cm^{-1} was observed by them.[23,24]

The computed $2J$ values for all the 10 isomers are summarized in Table 1. The isomers in which the radical moieties are coupled via one of the less sterically hindered connecting site "b" or "c" are observed to be anti-ferromagnetic in nature except the case of **c-d** isomer. On

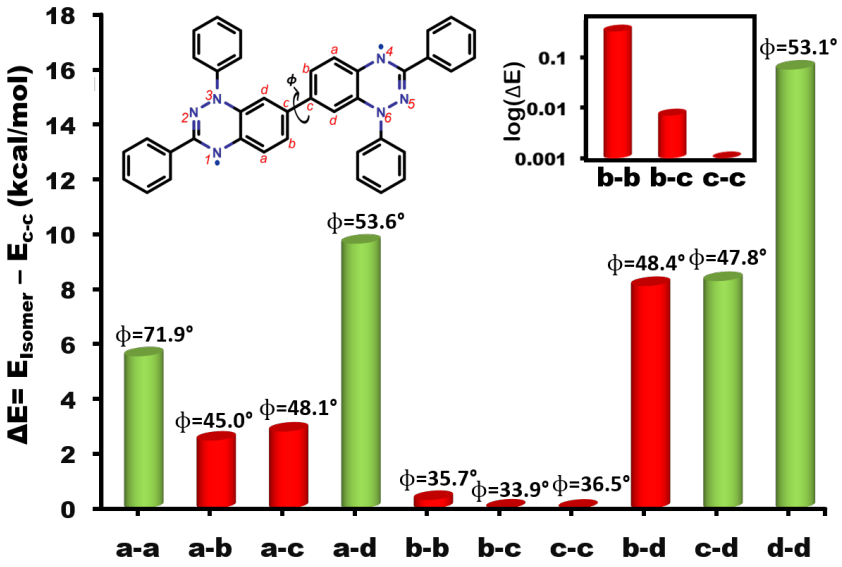

Figure 2: Relative energies (ΔE) of all the possible isomers of di-Blatter diradical, where ϕ is the dihedral angle between two monomeric units. The most sterically hindered isomers with large dihedral angle are the least stable. The inset of the graph shows the zoomed view of the energy difference between the isomers **b-b**, **b-c** and **c-c** at logarithmic scale. The red and green colored bars corresponds to anti-ferro and ferromagnetic exchange interactions respectively.

Table 1: Calculated magnetic exchange coupling constant $2J(\text{cm}^{-1})$ for all the 10 possible isomers of di-Blatter diradical.

Possible Isomers	$2J(cm^{-1})$			
	BS-DFT	CBS-DFT	CASSCF[a]	NEVPT2[a]
a-a	4.94	4.38	8.77	17.99
a-b	-162.70	-127.28	-32.48	-103.15
a-c	-168.10	-168.01	-25.02	-92.39
a-d	31.44	32.42	15.80	30.50
b-b	-196.36	-165.48	-79.42	-158.02
b-c	-262.38	-219.46	-100.73	-240.54
c-c[b]	-599.92	-544.28	-164.16	-511.60
b-d	-59.56	-49.16	-16.02	-12.57
c-d	29.30	33.78	11.85	38.84
d-d	10.20	9.48	2.41	7.46

[a] The calculations are performed using CAS(2,2) active space.
[b] Synthesized and reported $2J$ value is -444.19 cm^{-1}.[23,24]

contrary, small ferromagnetic exchange is obtained for the distorted isomers in which both the connections are made with the sterically hindered connecting sites "a" and "d" i.e. **a-a, a-d** and **d-d**. This variation of the nature of the magnetic exchange interactions with the connecting sites can also be seen from Fig. 2 where red and green bars denotes anti-ferro and ferromagnetic exchange respectively. The nature of exchange coupling is further verified by using various density and wave function-based multi-configurational methods and is found to be concordant. For the experimentally synthesized **c-c** isomer, a good match is obtained by using traditional BS-DFT, which further improves by constraining the appropriate amount of magnetic moment on the spatially confined zones in CBS-DFT. The detailed criteria for zone selection in CBS-DFT calculations is discussed in SI. CASSCF calculations with minimal active space, i.e. CAS(2,2) provides underestimated exchange coupling as compared to the experimental value of -444.19 cm^{-1} which improves significantly by the inclusion of dynamical correlation with NEVPT2 method.

In the following subsections, we will discuss the proposed *zonal spin alternation* rule. Followed by a comprehensive discussion, the origin of dominant anti-ferromagnetic exchange in the experimentally synthesized isomer **c-c** is provided. The ferromagnetic nature of the distorted diradicals originating from large torsional angles is addressed in the subsequent subsection.

3.1 Zonal spin alternation rule

The nature of magnetic exchange interactions and consequently the ground spin state can be visually predicted from the empirical *spin alternation* rule. This rule works perfectly well for the conjugated diradicals wherein the exchange takes place through bond.[45] However, the deviation from the *spin alternation* rule has been reported for sterically hindered cases where the large dihedral angle between the radical moieties breaks the electronic conjugation between π-orbitals and facilitates the direct exchange between the radical centres.[27,46] Such cases usually favors the parallel orientation of electrons residing in the p_z-orbitals of radical

centres following the Hund's Rule.[47] Thereby, apparently breaking the *spin alternation* rule and yielding ferromagnetic interactions.

Out of 10 possibilities of di-Blatter diradicals, the nature of magnetic exchange is in agreement with the *spin alternation* rule for six of the isomers. However, the ground spin state of the remaining four isomers, i.e., **a-a, a-b, b-c** and **d-d** is not supported by the *spin alternation* rule. The deviation from *spin alternation* rule is quite obvious for the rotated isomers **a-a** and **d-d** exhibiting large dihedral angles of 71.9° and 53.1° respectively. The observed ferromagnetic exchange in these rotated isomers is in accord to the Hund's rule. But, along with this, the dominant anti-ferromagnetic exchange interactions prevailing in the stable conjugated isomers is also found to be in contrast to the prediction of *spin alternation* rule for **a-b** and **b-c** isomers exhibiting small dihedral angles of 45.0° and 33.9° respectively. Thus, clearly indicating that the di-Blatter diradicals do not strictly follow the emperical *spin alternation* rule. The inadequacy of *spin alternation* rule for the di-Blatter diradicals could be foreseen from the spin density distribution of Blatter's monoradical, shown in Fig. 1b, which reveals an α spin density over the two consecutive N2 and N3 atoms. This is in complete contrast to the assumption of *spin alternation* rule where alternate signs of spin density are expected at the consecutive atoms. Thus, clearly revealing that the di-Blatter diradical exhibiting multiple spin centres forbids the simplest *spin alternation* rule.

As an alternative solution, we propose a modified version of *spin alternation* rule, called here as *zonal spin alternation* rule to correctly predict the nature of exchange interactions in such diradicals. The proposal of *zonal spin alternation* rule is based on the consideration of spatial zones exhibiting similar spin density on the constituent atoms. The contribution of individual atomic centres bearing alternate spin density in accord to *spin alternation* rule has been replaced by zones in *zonal spin alternation* rule. In Blatter's radical, all the atoms of the triazinyl and fused benzene ring exhibits α-spin density, thus triazinyl and fused benzene ring is taken as one complete entity (zone) bearing α-spin density and afterwards standard spin alternation rule is applied on individual atomic centres. The demonstration of *zonal*

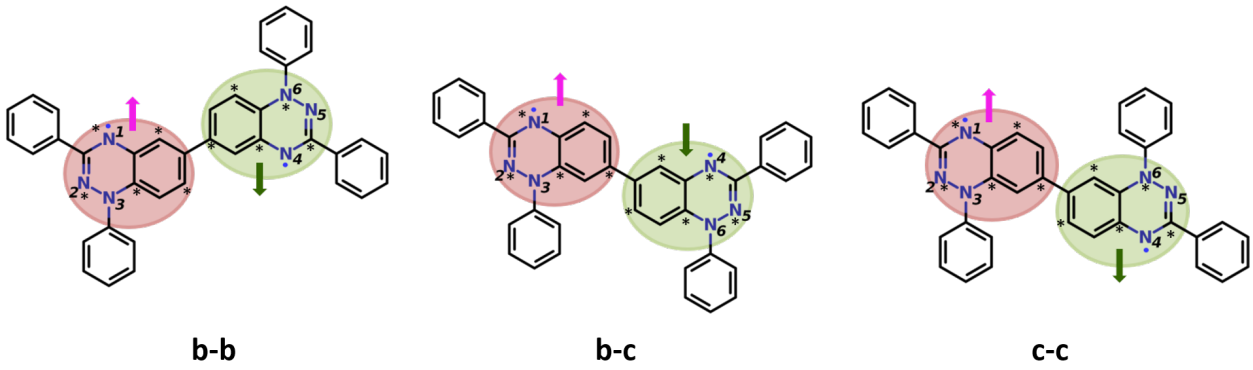

Figure 3: Three most stable and conjugated isomers of di-Blatter diradical, **b-b, b-c** and **c-c**. The pink and green circles over triazinyl and fused benzene ring denotes it as one complete zone bearing α and β-spin density respectively and the star-nonstar over the atomic centres depicts the notation of Ovchinnikov's rule

spin alternation is illustrated in Fig. 3 for the three most stable and conjugated isomers, **b-b, b-c** and **c-c**, wherein the triazinyl and fused benzene ring of Blatter's radical is considered as one complete entity with positive/negative spin-density denoted by pink/green circles. The star-nonstar convention over the atomic centres depicts the notation of the *spin alternation* and the similar *Ovchinnikov's* rules. This *zonal spin alternation* rule works perfectly well for the conjugated isomers of di-Blatter diradical as well as for reported Blatter's based diradicals.[20–22]

3.2 Multiple Pair-wise Exchange Interactions

To elucidate the origin of dominant anti-ferromagnetic exchange in stable isomers of di-Blatter diradical, we calculated the individual pair-wise exchange interactions between specific N-atoms. The spin density distribution of **c-c** isomer, illustrated in Fig. 4, reveals the existence of multiple spin centres in both singlet and triplet state. This scenario is in complete contrast with the much cultivated systems with only two magnetic centres and with only one magnetic exchange pathway. However, in di-Blatter diradical, due to strongly localized fractional magnetic moments that behave as independent micro-magnetic centres, there are total nine different possible pair-wise exchange interactions (i.e. $2J_{N1-N4}$, $2J_{N1-N5}$, $2J_{N1-N6}$, $2J_{N2-N4}$, $2J_{N2-N5}$, $2J_{N2-N6}$, $2J_{N3-N4}$, $2J_{N3-N5}$, $2J_{N3-N6}$ as shown in Fig. 5a).

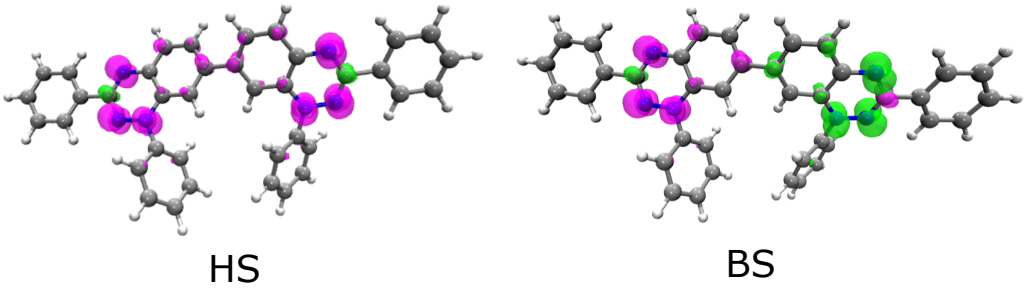

Figure 4: Spin-density distribution for diradical $\mathbf{c-c}$ in high-spin (HS) and broken-symmetry (BS) state. The α and β spins are shown in pink and yellow colours respectively with isovalue of 1×10^{-3} $\mu_B/Å^3$. All the six N-atoms exhibits approximate 0.23 μ_B spin moment in both HS and BS state with the sign reversal in BS state.

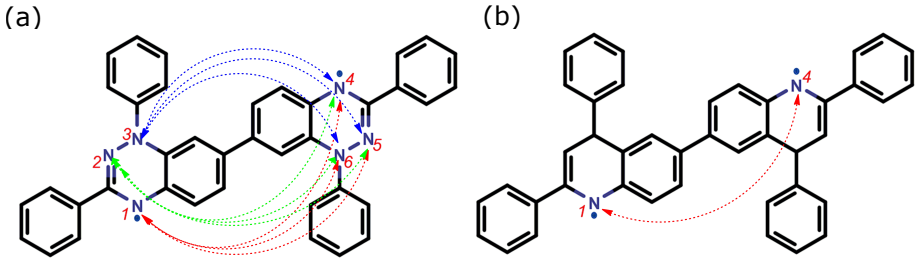

Figure 5: **(a)**Different possible interactions in isomer **c-c** ($2J_{Nx-Ny}$ (x= 1,2,3 and y=4,5,6)). The interaction of N1, N2, N3 with N4-N6 is denoted by *red, green* and *blue* color respectively, **(b)** Diradical $\mathbf{cc_1}$ to compute the individual exchange interaction between N1 and N4 ($2J'_{N1-N4}$).

In order to have a proper description of exchange coupling in di-Blatter diradical with multiple magnetic centres, the exchange coupling constants between specific N-pairs are estimated while keeping all other paramagnetic N-atoms magnetically inactive by replacing N-atoms with isoelectronic CH-units in the triazinyl rings. For example, to determine exchange interactions between N1 and N4 i.e. $\mathbf{2}J_{\mathbf{N1-N4}}$ in **c-c** isomer, all the other N-atoms except N1 and N4 are replaced by CH-units as shown in Fig. 5b (denoted as $\mathbf{cc_1}$) and the obtained coupling constant is denoted by $\mathbf{2}J'_{\mathbf{N1-N4}}$. As expected, the replacement of N-atoms by CH-units increases the spin density on more electronegative N1 and N4 atoms of diradical $\mathbf{cc_1}$ which results in overestimated exchange , i.e. $\mathbf{2}J'_{\mathbf{N1-N4}}$. Thus, in a refined treatment, the exact exchange between N1 and N4, $\mathbf{2}J_{\mathbf{N1-N4}}$, is obtained by augmentation of the obtained $\mathbf{2}J'_{\mathbf{N1-N4}}$ with the ratio of spin densities deduced from diradical **c-c** and $\mathbf{cc_1}$ respectively. The values of $\mathbf{2}J_{\mathbf{N1-N4}}$ and $\mathbf{2}J'_{\mathbf{N1-N4}}$ are approximated with BS-DFT calculations.

Similarly, the exchange coupling for all the possible 9 magnetic interactions i.e. $2J_{Nx-Ny}$ (x= 1,2,3 and y=4,5,6) shown in Fig. 5a are evaluated (can be found in SI). The total $2J$ is obtained as the weighted summation of all the calculated $2J$'s between different magnetic sites. This methodology of calculating individual pairwise magnetic exchange interactions again provides anti-ferromagnetic exchange which is concordant with predicted nature of exchange interactions using all the DFT and wave function-based methods. Although, among all 9 possibilities, both ferromagnetic and anti-ferromagnetic individual pairwise interactions strictly following the spin alternation rule prevailed between two N-atoms, but the magnitude of anti-ferromagnetic interactions was found to be dominating over the ferromagnetic. Thus giving resultant anti-ferromagnetic exchange for isomer **c-c**. Similarly, all the 9 possible exchange interactions are calculated for isomer **b-b** and **b-c** and are provided in SI. An anti-ferromagnetic exchange is found to be dominating in both the isomers as well.

3.3 Switching of Magnetic Exchange Interactions

The detailed analysis of individual pairwise interactions provides clear signatures of a strong anti-ferromagnetic exchange in planar isomers with connecting sites "b" and "c". However, small ferromagnetic exchange is observed for non-planar sterically hindered isomers with connecting sites "a" and "d" i.e., **a-a, a-d, c-d** and **d-d**. The effect of dihedral angle in controlling the magnetic exchange interactions is well documented in literature.[48–50] Shil et al. also postulated that in the crowded forms with large dihedral angles, the itinerant exchange between two magnetic sites through π network is forbidden due to non-planarity.[46] In such diradicals, the radical sites being closer in space participate in direct exchange, which usually favors the ferromagnetic coupling following the Hund's rule.[47]

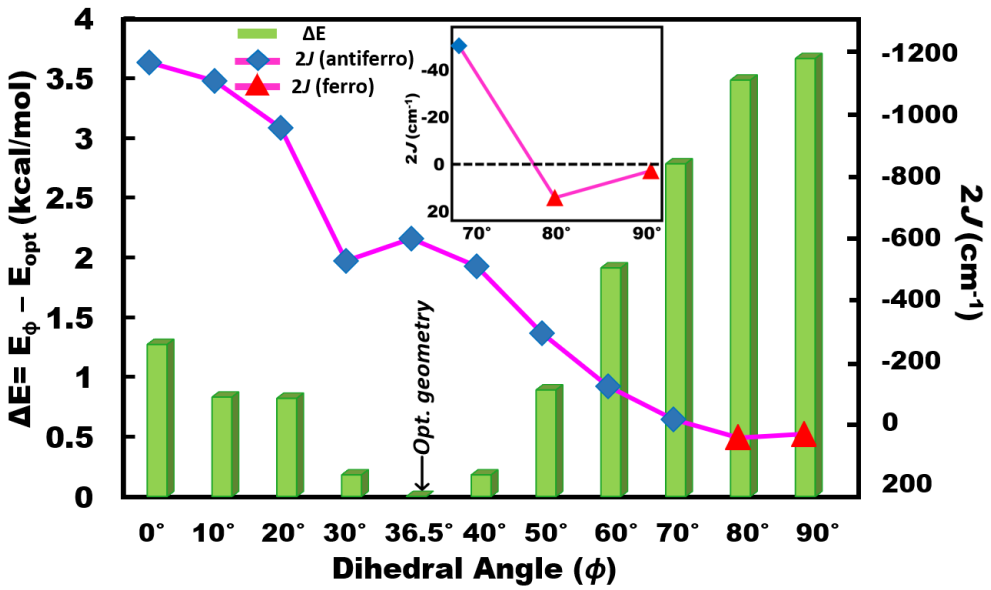

Figure 6: Relative energies (ΔE) and variation of exchange coupling constant ($2J$) with dihedral angle between two radical monomers for **c-c** isomer. The green bars represents relative energies calculated at B3LYP/def2-TZVP level. The ferro and anti-ferro exchange is denoted by red triangles and blue diamonds respectively over pink curve.

To validate whether the weak ferromagnetic exchange interaction in the sterically hindered isomers is indeed a direct effect of dihedral angle, we computed the exchange interactions for **c-c** isomer by constraining the dihedral angle (ϕ) between two monomeric units

and further varying ϕ from 0 to 90°. The variation of $2J$ with dihedral angle, illustrated in Fig. 6 by a pink curve, clearly reveals that the planar geometry with small dihedral angles (including the optimized one at 36.5°) favors anti-ferromagnetic exchange. However, on approaching the orthogonal orientation at ∼80°, the nature of the exchange between two radical monomers switches to ferromagnetic (also illustrated in the inset of Fig. 6). Along with this, the relative energies, represented by green bars in Fig. 6, reveals that sterically hindered geometries with large dihedral angles are least stable. Similar behavior is observed for sterically hindered isomer **a-a** yielding ferromagnetic exchange at optimized dihedral 71.89° while switching to anti-ferromagnetic exchange on constraining the dihedral to 50° (data is provided in SI).

Thus, as revealed from multiple pair-wise exchange interactions, due to co-existing multiple micro-magnetic centres, anti-ferromagnetic interactions are much dominating in di-Blatter diradicals. However, switching to weak ferromagnetic exchange in strained isomers as well as in rotated configurations indicates that one can obtain ferromagnetic exchange in the super-stable diradicals by tuning the dihedral angle.

4 Conclusions

The magnetic exchange interactions are investigated for all the possible isomers of di-Blatter diradical adopting various density as well as wave function-based multi-configurational methods. It reveals coupling the two Blatter's radicals via fused benzene ring yield an anti-ferromagnetic exchange in their stable conjugated configurations. A close agreement with the experimental observations are obtained using traditional DFT based broken symmetry methods, which further improves by employing CBS-DFT. It has been realized that the minimal CAS space accounting two unpaired electrons in two magnetic orbitals, when considered along with dynamical correlations, i.e., CASSCF(2,2)-NEVPT2, provides a reasonable choice to compute exchange interaction in di-Blatter diradicals.

Further, due to α-spin density on all the three N-atoms of Blatter's radical, it forbids the simplest *spin alternation* rule. However, the nature of magnetic exchange interactions in all the Blatter's based conjugated diradicals can be explained accurately by the proposed *zonal spin alternation* rule. Due to the existence of multiple spin centres, di-Blatter diradicals exhibits numerous exchange pathways. In the conjugated stable isomers, the dominating micro-magnetic exchange interactions dictate the magnetic properties of the diradical i.e. anti-ferromagnetic interactions. However, in certain strained isomers as well as in rotated configurations the exchange interactions switch from anti-ferro to weak ferromagnetic interactions. Thus, in-principle switching occurs in a trade-off with molecular stability, hence, synthesizing a ferromagnetically coupled di-Blatter diradical remains as a possibility but a challenging task.

Acknowledgement

The authors thank Jayamurugan G for various helpful discussions. RK thanks CSIR, India for the JRF fellowship with grant no. 09/1129(0016)/2019-EMR-I. Financial support from Department of Science and Technology through SERB-ECR project No. ECR/2016/000362, India-Sweden joint project No. DST/INT/SWD/VR/P-01/2016.

Supporting Information Available: Computed total energies, zone selection criteria for CBS-DFT calculations, selection of active space for CASSCF calculations, magnetic exchange couplings for individual pairwise interactions, variation of $2J$ with dihedral angle. This material is available free of charge via the Internet at http:// pubs.acs.org.

References

(1) Datta, S. N.; Trindle, C.; Illas, F. *Theoretical and computational aspects of magnetic organic molecules*; World Scientific, 2014.

(2) Ratera, I.; Veciana, J. Playing with organic radicals as building blocks for functional molecular materials. *Chem. Soc. Rev.* **2012**, *41*, 303–349.

(3) Wolf, S.; Awschalom, D.; Buhrman, R.; Daughton, J.; Von Molnar, S.; Roukes, M.; Chtchelkanova, A. Y.; Treger, D. Spintronics: a spin-based electronics vision for the future. *Science* **2001**, *294*, 1488–1495.

(4) Hu, X.; Wang, W.; Wang, D.; Zheng, Y. The electronic applications of stable diradicaloids: present and future. *J. Mater. Chem. C* **2018**, *6*, 11232–11242.

(5) Sanvito, S. Molecular spintronics. *Chem. Soc. Rev.* **2011**, *40*, 3336–3355.

(6) Hicks, R. G. What's new in stable radical chemistry? *Org. Biomol. Chem.* **2007**, *5*, 1321–1338.

(7) Vela, S.; Reardon, M. B.; Jakobsche, C. E.; Turnbull, M. M.; Ribas-Arino, J.; Novoa, J. J. Bistability in Organic Magnetic Materials: A Comparative Study of the Key Differences between Hysteretic and Non-hysteretic Spin Transitions in Dithiazolyl Radicals. *Chem.: Eur. J* **2017**, *23*, 3479–3489.

(8) Gilroy, J. B.; McKinnon, S. D.; Kennepohl, P.; Zsombor, M. S.; Ferguson, M. J.; Thompson, L. K.; Hicks, R. G. Probing electronic communication in stable benzene-bridged verdazyl diradicals. *J. Org. Chem.* **2007**, *72*, 8062–8069.

(9) Abe, M. Diradicals. *Chem. Rev.* **2013**, *113*, 7011–7088.

(10) Blatter, H. M.; Lukaszewski, H. A new stable free radical. *Tetrahedron Lett.* **1968**, *9*, 2701–2705.

(11) Constantinides, C. P.; Koutentis, P. A.; Krassos, H.; Rawson, J. M.; Tasiopoulos, A. J. Characterization and Magnetic Properties of a "Super Stable" Radical 1, 3-Diphenyl-7-trifluoromethyl-1, 4-dihydro-1, 2, 4-benzotriazin-4-yl. *J. Org. Chem.* **2011**, *76*, 2798–2806.

(12) Kaszyński, P.; Constantinides, C. P.; Young Jr, V. G. The Planar Blatter Radical: Structural Chemistry of 1, 4-Dihydrobenzo [e][1, 2, 4] triazin-4-yls. *Angew. Chem.* **2016**, *55*, 11149–11152.

(13) Bazzi, F.; Danke, A. J.; Lawson, D. B.; Manoli, M.; Leitus, G.; Koutentis, P. A.; Constantinides, C. P. 1-(2-Methoxyphenyl)-3-(phenyl)-1, 4-dihydro-1, 2, 4-benzotriazin-4-yl: A Tricky "Structure-to-Magnetism" Correlation Aided by DFT Calculations. *CrystEngComm* **2020**,

(14) Ciccullo, F.; Gallagher, N.; Geladari, O.; Chassé, T.; Rajca, A.; Casu, M. A derivative of the Blatter radical as a potential metal-free magnet for stable thin films and interfaces. *ACS Appl. Mater. Interfaces* **2016**, *8*, 1805–1812.

(15) Low, J. Z.; Kladnik, G.; Patera, L. L.; Sokolov, S.; Lovat, G.; Kumarasamy, E.; Repp, J.; Campos, L. M.; Cvetko, D.; Morgante, A. et al. The Environment-Dependent Behavior of the Blatter Radical at the Metal–Molecule Interface. *Nano Lett.* **2019**, *19*, 2543–2548.

(16) Patera, L. L.; Sokolov, S.; Low, J. Z.; Campos, L. M.; Venkataraman, L.; Repp, J. Resolving the Unpaired-Electron Orbital Distribution in a Stable Organic Radical by Kondo Resonance Mapping. *Angew. Chem. Int. Ed.* **2019**, *58*, 11063–11067.

(17) Sidharth, T. N. S.; Nasani, R.; Gupta, A.; Sooraj, B. N. S.; Roy, S.; Mondal, A.; Konar, S. Reversal of magnetic exchange coupling between copper (II) and Blatter radical depending on the coordination environment. *Inorganica Chim. Acta* **2020**, *503*, 119395.

(18) Bartos, P.; Young Jr, V. G.; Kaszyński, P. Ring-Fused 1, 4-Dihydro [1, 2, 4] triazin-4-yls through Photocyclization. *Org. Lett.* **2020**, *22*, 3835–3840.

(19) Areephong, J.; Mattson, K.; Treat, N.; Poelma, S.; Kramer, J.; Sprafke, H.; Latimer, A.; de Alaniz, J. R.; Hawker, C. Triazine-mediated controlled radical polymerization: new unimolecular initiators. *Polym. Chem.* **2016**, *7*, 370–374.

(20) Gallagher, N. M.; Bauer, J. J.; Pink, M.; Rajca, S.; Rajca, A. High-spin organic diradical with robust stability. *J. Am. Chem. Soc.* **2016**, *138*, 9377–9380.

(21) Gallagher, N.; Zhang, H.; Junghoefer, T.; Giangrisostomi, E.; Ovsyannikov, R.; Pink, M.; Rajca, S.; Casu, M. B.; Rajca, A. Thermally and Magnetically Robust Triplet Ground State Diradical. *J. Am. Chem. Soc.* **2019**, *141*, 4764–4774.

(22) Bajaj, A.; Ali, M. E. First Principle Designing of Blatter's Diradicals with Strong Ferromagnetic Exchange Interactions. *J. Phys. Chem. C* **2019**, *123*, 15186–15194.

(23) Hu, X.; Chen, H.; Zhao, L.; Miao, M.; Han, J.; Wang, J.; Guo, J.; Hu, Y.; Zheng, Y. Nitrogen analogues of Chichibabin's and Müller's hydrocarbons with small singlet–triplet energy gaps. *Chem. Commun.* **2019**, *55*, 7812–7815.

(24) Hu, X.; Chen, H.; Xue, G.; Zheng, Y. Correlation between the strength of conjugation and spin–spin interactions in stable diradicaloids. *J. Mater. Chem. C* **2020**, doi: 10.1039/d0tc00868k.

(25) Stuyver, T.; Chen, B.; Zeng, T.; Geerlings, P.; De Proft, F.; Hoffmann, R. Do Diradicals Behave Like Radicals? *Chem. Rev.* **2019**, *119*, 11291–11351.

(26) Trindle, C.; Datta, S. N. Molecular orbital studies on the spin states of nitroxide species: Bis-and trisnitroxymetaphenylene, 1, 1-bisnitroxyphenylethylene, and 4, 6-dimethoxy-1, 3-dialkylnitroxy-benzenes. *Int. J. Quantum Chem.* **1996**, *57*, 781–799.

(27) Pal, A. K.; Mañeru, D. R.; Latif, I. A.; de PR Moreira, I.; Illas, F.; Datta, S. N. Theoretical and computational investigation of meta-phenylene as ferromagnetic coupler in nitronyl nitroxide diradicals. *Theor. Chem. Acc.* **2014**, *133*, 1472.

(28) Ali, M. E.; Datta, S. N. Broken-symmetry density functional theory investigation on bis-nitronyl nitroxide diradicals: influence of length and aromaticity of couplers. *J. Phys. Chem. A* **2006**, *110*, 2776–2784.

(29) Fang, S.; Lee, M.-S.; Hrovat, D. A.; Borden, W. T. Ab initio calculations show why m-phenylene is not always a ferromagnetic coupler. *J. Am. Chem. Soc.* **1995**, *117*, 6727–6731.

(30) Ovchinnikov, A. A. Multiplicity of the ground state of large alternant organic molecules with conjugated bonds. *Theor. Chim. Acta* **1978**, *47*, 297–304.

(31) Noodleman, L. Valence bond description of antiferromagnetic coupling in transition metal dimers. *J. Chem. Phys.* **1981**, *74*, 5737–5743.

(32) Kaduk, B.; Kowalczyk, T.; Van Voorhis, T. Constrained density functional theory. *Chem. Rev.* **2012**, *112*, 321–370.

(33) Nair, N. N.; Schreiner, E.; Pollet, R.; Staemmler, V.; Marx, D. Magnetostructural dynamics with the extended broken symmetry formalism: Antiferromagnetic [2Fe-2S] complexes. *J. Chem. Theory Comput.* **2008**, *4*, 1174–1188.

(34) Ali, M. E.; Nair, N. N.; Staemmler, V.; Marx, D. Constrained spin-density dynamics of an iron-sulfur complex: Ferredoxin cofactor. *J. Chem. Phys.* **2012**, *136*, 224101.

(35) Reta Mañeru, D.; Pal, A. K.; Moreira, I. d. P.; Datta, S. N.; Illas, F. The Triplet–Singlet Gap in the m-Xylylene Radical: A Not So Simple One. *J. Chem. Theory Comput.* **2013**, *10*, 335–345.

(36) Illas, F.; Moreira, I. P.; De Graaf, C.; Barone, V. Magnetic coupling in biradicals, binuclear complexes and wide-gap insulators: a survey of ab initio wave function and density functional theory approaches. *Theor. Chem. Acc.* **2000**, *104*, 265–272.

(37) Shil, S.; Herrmann, C. Performance of range-separated hybrid exchange–correlation functionals for the calculation of magnetic exchange coupling constants of organic diradicals. *J. Comput. Chem.* **2018**, *39*, 780–787.

(38) Neese, F. The ORCA program system. *Wiley Interdiscip. Rev. Comput. Mol. Sci.* **2012**, *2*, 73–78.

(39) Valiev, M.; Bylaska, E. J.; Govind, N.; Kowalski, K.; Straatsma, T. P.; Van Dam, H. J.; Wang, D.; Nieplocha, J.; Apra, E.; Windus, T. L. et al. NWChem: A comprehensive and scalable open-source solution for large scale molecular simulations. *Comput. Phys. Commun.* **2010**, *181*, 1477–1489.

(40) Angeli, C.; Pastore, M.; Cimiraglia, R. New perspectives in multireference perturbation theory: the n-electron valence state approach. *Theor. Chem. Acc.* **2007**, *117*, 743–754.

(41) Barone, V.; Cacelli, I.; Ferretti, A. The role of the multiconfigurational character of nitronyl-nitroxide in the singlet–triplet energy gap of its diradicals. *Phys. Chem. Chem. Phys.* **2018**, *20*, 18547–18555.

(42) Ali, M. E.; Staemmler, V.; Illas, F.; Oppeneer, P. M. Designing the redox-driven switching of ferro-to antiferromagnetic couplings in organic diradicals. *J. Chem. Theory Comput.* **2013**, *9*, 5216–5220.

(43) Suaud, N.; Ruamps, R.; Guihéry, N.; Malrieu, J.-P. A strategy to determine appropriate active orbitals and accurate magnetic couplings in organic magnetic systems. *J. Chem. Theory Comput.* **2012**, *8*, 4127–4137.

(44) Malrieu, J. P.; Caballol, R.; Calzado, C. J.; de Graaf, C.; Guihéry, N. Magnetic interactions in molecules and highly correlated materials: physical content, analytical derivation, and rigorous extraction of magnetic Hamiltonians. *Chem. Rev.* **2014**, *114*, 429–492.

(45) Song, M.; Song, X.; Bu, Y. Tuning the Spin Coupling Interactions in the Nitroxide-Based Bisphenol-Like Diradicals. *ChemPhysChem* **2017**, *18*, 2487–2498.

(46) Shil, S.; Misra, A. Photoinduced antiferromagnetic to ferromagnetic crossover in organic systems. *J. Phys. Chem. A* **2009**, *114*, 2022–2027.

(47) Sinha, B.; Ramasesha, S. Direct versus kinetic exchange in multiband models for organic ferromagnetism. *Phys. Rev. B* **1993**, *48*, 16410.

(48) Ali, M. E.; Roy, A. S.; Datta, S. N. Molecular tailoring and prediction of strongly ferromagnetically coupled trimethylenemethane-based nitroxide diradicals. *J. Phys. Chem. A* **2007**, *111*, 5523–5527.

(49) Ko, K. C.; Cho, D.; Lee, J. Y. Systematic approach to design organic magnetic molecules: strongly coupled diradicals with ethylene coupler. *J. Phys. Chem. A* **2012**, *116*, 6837–6844.

(50) Faust, T. B.; Tuna, F.; Timco, G. A.; Affronte, M.; Bellini, V.; Wernsdorfer, W.; Winpenny, R. E. Controlling magnetic communication through aromatic bridges by variation in torsion angle. *Dalton Trans.* **2012**, *41*, 13626–13631.

Graphical TOC Entry